Determination of B-site ordering and structural transformations in the mixed transition metal perovskites La_2CoMnO_6 and La_2NiMnO_6

2003 J. Phys.: Condens. Matter 15 4927

(http://iopscience.iop.org/0953-8984/15/29/304)

INSTITUTE OF PHYSICS PUBLISHING JOURNAL OF PHYSICS: CONDENSED MATTER

J. Phys.: Condens. Matter **15** (2003) 4927–4936 PII: S0953-8984(03)55455-8

Determination of B-site ordering and structural transformations in the mixed transition metal perovskites La_2CoMnO_6 and La_2NiMnO_6

C L Bull[1], **D Gleeson**[1] **and K S Knight**[2,3]

[1] Davy Faraday Research Laboratories, The Royal Institution of Great Britain, 21 Albemarle Street, London W1S 4BS, UK
[2] ISIS Pulsed Neutron and Muon Source, Rutherford Appleton Laboratories, Chilton, Didcot, Oxon OX11 0QX, UK
[3] Department of Mineralogy, The Natural History Museum, Cromwell Road, London SW7 5BD, UK

E-mail: craig@ri.ac.uk

Received 1 November 2002, in final form 17 June 2003
Published 11 July 2003
Online at stacks.iop.org/JPhysCM/15/4927

Abstract

The low- and high-temperature structures of La_2CoMnO_6 and La_2NiMnO_6 have been refined using powder neutron diffraction. At low temperatures the materials adopt a charge-ordered monoclinic structure which transforms to a rhombohedral structure at elevated temperature without loss of charge ordering. This charge ordering scheme allows us for the first time to rationalize the relationships between the physical and structural properties of these materials.

1. Introduction

Perovskites are an important class of materials, characterized by subtle structural distortions from the cubic aristotype structure. The distortions are caused by concerted rotations of the BO_6 octahedra and displacements of the A and B cations within the cage. These distortions are temperature and pressure dependent. These distortions give rise to dramatic changes in properties such as dielectric properties, electrical resistivity and band gap. These important materials have received a large amount of academic interest and have potential applications in catalysis, magnetic media, electrical conductors and gas sensors.

We have investigated the structural and physical properties of La_2CoMnO_6 and La_2NiMnO_6 and have been able to derive structure–property relationships as detailed elsewhere [1, 2]. Although these materials have been investigated previously [3], the reported crystal structures do not account for their physical properties. Previous work has incorrectly identified the structure of these materials as either pseudo cubic [4–6] or orthorhombic [7]. Furthermore, it has also been suggested by Goodenough *et al* [8] that the materials are biphasic with the coexistence of a rhombohedral and orthorhombic phase. The reported orthorhombic or

pseudo-cubic structures do not permit the transition metal (TM) ions to be ordered as they only contain one symmetry-independent octahedral site. Ordering of the TM cations could account for the anomalies observed in the electrical properties of our materials [1, 2]. The measured electrical conductivities are less than expected when compared to the conductivities of the parent materials ($LaMnO_3$, $LaCoO_3$ and $LaNiO_3$). Charge ordering can cause localization of the electrons and may render it either insulating or semiconducting. It has been shown previously that charge ordering occurs when TM ions (in different oxidation states) are located on separate, specific lattice sites in a mixed valence material [9].

The reported structural models also show discrepancies in the TM–O bond distances derived from extended x-ray absorption fine structure (EXAFS) which show distinct TM–O distances for Co/Mn in La_2CoMnO_6 and Ni/Mn in La_2NiMnO_6 [1, 2]. Indeed, Asai *et al* [10] suggested that the symmetry should be monoclinic while the diffraction pattern could only be indexed as orthorhombic ($Pnma$, no 62). They performed a Rietveld analysis on x-ray data of an assumed cation ordered La_2CoMnO_6 in the space group $P2_1/c$. They were only able to obtain accurate rare earth positions which could be due to both the low scattering power of oxygen compared to the lanthanide [11] and the inability of the technique to distinguish between the two different TM ions due to their similar x-ray scattering factors. Resonant (anomalous) powder x-ray diffraction could not be used in our study due to the similar absorption energies of the TM atoms in both materials. Thus, we have used neutron diffraction to ascertain a structure for both materials as the scattering lengths for Mn, Co and Ni are substantially different and in addition oxygen has a large scattering length (Mn—3.73 fm, Ni—10.3 fm, Co—2.49 fm and O—5.803 fm) [12]. The structural information gained from this study has allowed us to determine the presence of cation ordering within these materials and to assign oxidation states to the TM ions. The assignment of the formal oxidation states of the TM ions in these materials has also been a source of debate over the years. Previous workers have suggested Ni/Co as +2 and Mn as +4 or Ni/Co as +3 and Mn as +3 [13–15]. We also show, for the first time to our knowledge, a high-temperature structural transition from monoclinic to rhombohedral in both compounds in which the cation ordering scheme is retained.

2. Experimental details

Monophasic, crystalline samples of La_2CoMnO_6 and La_2NiMnO_6 were prepared by a modified nitrate decomposition route [16]. The metal nitrates (Aldrich 99.99%) in the appropriate ratios were dissolved in water and then heated in a crucible of known weight to 130 °C to remove the water. The residual brown solid was then decomposed to oxides at 600 °C for 30 min with the evolution of NO_2, and finally heated to 1100 °C at a rate of 10 °C min^{-1} for 16 h to react the oxides before cooling at a rate of 1 °C min^{-1} to room temperature. The material was then ground and pressed into a pellet before repeating the final heating cycle several times until no further improvements in crystallinity were observed by comparison of the width of the peaks in the x-ray diffraction pattern. The oxygen content of the materials was determined by calculating the changes in weight in the sample after each stage of the heating process.

The degree of crystallinity and phase purity of each of the materials was determined by x-ray diffraction using a Siemens D5000 diffractometer using Cu Kα_1 radiation selected using a graphite monochromator. Differential scanning calorimetry (DSC) was carried out with a Shimadzu DSC-50 using Pt crucibles and alumina as the reference. The samples were heated in an atmosphere of oxygen or nitrogen over a temperature range of 20–600 °C with a ramp rate of 10 °C min^{-1}.

Time-of-flight (TOF) neutron diffraction experiments were undertaken on beam line S8 using the HRPD station located at the ISIS Neutron Spallation Source, Rutherford Appleton

Laboratory (RAL), Chilton, Didcot, UK. The sample was loaded into a 12 mm diameter vanadium canister mounted in a vanadium tailed resistance furnace with a cylindrical vanadium element and heat shields. Vanadium was used throughout due to its small coherent scattering length, giving negligible contaminant lines in the powder pattern. The diffraction pattern was collected using the backscattering detector over a TOF range of 30–130 ms, corresponding to a d-spacing of 0.6–2.6 Å with a typical collection time of 12 h. Diffraction patterns were collected at room temperature and 25 °C either side of the exothermic transitions observed in the DSC for each of the samples.

The raw data were then focused and the contribution to the background resulting from the furnace was removed using the in-house software at RAL. Rietveld profile analysis was then undertaken using the GSAS suite of programs [17].

3. Results

3.1. Room-temperature diffraction

Powder x-ray diffraction (XRD) confirmed the materials to be monophasic. The first 25 peaks were used in the indexing program TREOR which suggested an orthorhombic unit cell [18]. The occurrence of the systematic absences suggested the orthorhombic space group $Pnma$ (no 62). The data were initially fitted using the Le Bail extraction method [19] which refines the diffraction profile without a structural model. This quickly converged with a χ^2 of 4.13. A pseudo-Voigt function was used to describe the peak shape and a shifted Chebyshev polynomial background with four coefficients was used in each case. Subsequently a Rietveld refinement was undertaken using the orthorhombic structure of $LaMnO_3$ and the profile coefficients from the Le Bail extraction as the starting point [20]. Rietveld refinement for materials of the type $LnTMO_3$ in the $Pnma$ space group only allows a single, mixed TM site and hence yields an averaged TM–oxygen distance which does not allow the determination of the presence of (or degree of) charge ordering or the assignment of oxidation states. Within experimental error the oxygen content determined by mass changes during the synthesis was found to be as suggested by the chemical formula.

By contrast the room-temperature neutron data could not be indexed in the same orthorhombic cell. Indeed, the splitting of the peak at 2.25 Å, shown in figure 1, and the violation of the systematic absences of $Pnma$ indicated a reduction of the symmetry to monoclinic. Le Bail pattern decompositions were then undertaken for each of the potential monoclinic space groups which indicated that the material was best described in the monoclinic space group $P2_1/n$ (unique axis b, no 14) on the basis that this gave the lowest value of χ^2. The reduction in symmetry to $P2_1/n$ allowed for the possibility of distinct sites for the different TM ions (Wyckoff positions 2c and 2b). The peak profile was fitted with the model of David and von Dreele [17, 21], which incorporates the moderator pulse shape of Ikeda and Carpenter [22], and the background fitted using a shifted Chebyshev polynomial with 10 coefficients. The initial unit cell parameters were obtained by transformation from those determined by x-ray diffraction in the $Pnma$ space group. The initial atomic positions used for the subsequent Rietveld refinement were obtained from the theoretical model of Woodward which assumes that octahedral tilting exists within the perovskite structure [23]. Initially the fractional occupancies of the two TM sites were defined as 50% Mn and 50% Co or Ni in accordance with the structure determined from XRD. The atomic positions, fractional occupancies, lattice parameters and isotropic displacement parameters of all the atoms were then refined to convergence. The sum of the occupancies of the individual TM sites was constrained to be unity throughout the refinement. In the initial stages of the refinement,

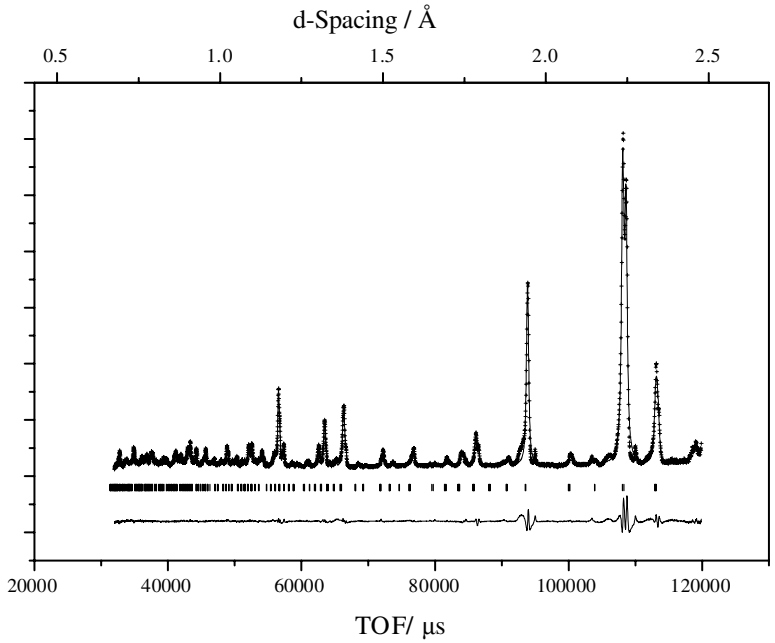

Figure 1. The neutron observed (+) and calculated (——) profile and difference profiles (bottom trace) for La_2CoMnO_6 at 25 °C.

the isotropic displacement parameters of similar atom types were constrained to be equal; however, these were then allowed to refine freely along with the coefficients of the background and profile in the latter stages of the refinement. Finally, the absorption and DIFA coefficients were refined to correct for the absorption of the neutrons by the sample and its affect on the apparent flight path. A significant observation from the analysis is the presence of cation ordering in both compounds.

The observed, calculated and difference profiles for the calculated structures for La_2CoMnO_6 and La_2NiMnO_6 at ambient temperature are given in figures 1 and 2 respectively. The unit cell parameters, atomic positions, thermal parameters and structure refinement details are given in table 1. Selected interatomic distances and angles are given in table 2.

3.2. High-temperature diffraction

DSC showed large exothermic transitions at 325 and 375 °C for La_2CoMnO_6 and La_2NiMnO_6 respectively. Neutron diffraction patterns were then collected at 25 °C either side of these transitions in order to understand the nature of these transitions. The diffraction patterns obtained above the transition temperature showed significant changes in intensity of the peaks at 2.25 Å (figure 3). The first 25 peaks were then used in the indexing program TREOR [18] which suggested a rhombohedral unit cell. The temperature of the exotherm in the DSC was to be explained in terms of cation migration leading to TM site averaging. Thus, as we found the first phase to be charge ordered, we were led to the choice of the $R\bar{3}$ space group (no 148) in the rhombohedral setting over the $R\bar{3}c$ space group (no 167) which would require full cation disordering. The data were then fitted using the Le Bail method [19] as described previously for the low-temperature refinements. The initial unit cell parameters were taken from our earlier high-temperature x-ray diffraction study [1]. The initial atomic positions used for the subsequent Rietveld refinement were obtained from the theoretical models of Woodward [23]

Table 1. Results of Rietveld refinement of neutron diffraction data for La_2NiMnO_6 and La_2CoMnO_6 at ambient temperature.

Parameter	La_2NiMnO_6	La_2CoMnO_6
Space group	$P2_1/n$	$P2_1/n$
a (Å)	5.467 038(34)	5.525 192(18)
b (Å)	5.510 480(31)	5.487 598(13)
c (Å)	7.751 242(36)	7.778 682(25)
α (deg)	90	90
β (deg)	90.1199(9)	89.9495(6)
γ (deg)	90	90
La x	0.002 142(11)	0.007 21(7)
y	0.0522(13)	0.023 95(5)
z	0.262 90(7)	0.244 42(11)
U_{iso} (Å^2)	0.004 51(11)	0.000 44(7)
Co/Ni x	0	0
y	0.5	0.5
z	0	0
U_{iso} (Å^2)	0.028 67(17)	0.055 48(13)
Mn x	0.5	0.5
y	0	0
z	0	0
U_{iso} (Å^2)	0.028 67(17)	0.002 12(4)
O1 x	0.250 58(13)	0.289 38(16)
y	0.234 70(14)	0.265 40(12)
z	0.231 50(14)	0.034 78(16)
U_{iso} (Å^2)	0.0576(10)	0.081 62(31)
O2 x	0.294 32(13)	0.264 56(16)
y	0.292 83(14)	0.275 34(25)
z	0.474 74(18)	0.463 17(18)
U_{iso} (Å^2)	0.005 53(10)	0.009 32(41)
O3 x	0.543 43(32)	0.570 22(8)
y	0.036 07(34)	−0.001 92 (9)
z	0.243 02(26)	0.243 66(23)
U_{iso} (Å^2)	0.00771 (10)	0.007 39(15)
Co/Ni:Mn ordering (%)	85	90
R_p(%)	6.93	8.76
wR_p(%)	9.02	10.24
χ^2	15.02	18.11

for an ordered system (in an indexed space group). To test for any cation migration the fractional occupancies of the two TM sites were given initial values of 50% Mn and 50% Co or Ni corresponding to a fully disordered model. The atomic positions, fractional occupancies, lattice parameters and isotropic displacement parameters of all the atoms were then refined to convergence. The sum of the occupancies of the individual TM sites was constrained to be unity throughout the refinement. In the initial stages of the refinement, the isotropic displacement of similar atom types was constrained to be equal. However, these were allowed to refine freely along with the coefficients of the background and profile and the timing uncertainty in the final stages of the refinement. The observed, calculated and difference profiles for the calculated structures for La_2CoMnO_6 at 350 °C and La_2NiMnO_6 at 400 °C are given in figures 3 and 4

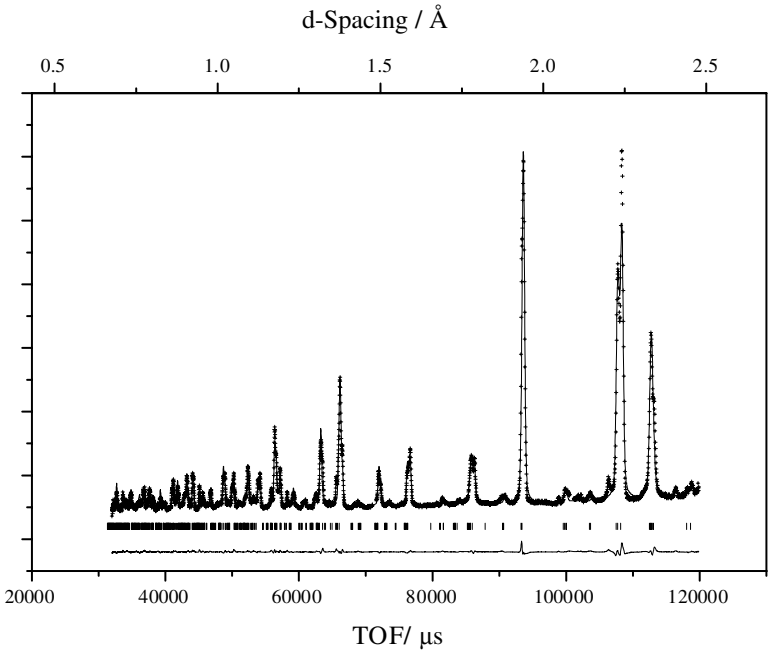

Figure 2. The neutron observed (+) and calculated (——) profile and difference profiles (bottom trace) for La_2NiMnO_6 at 25 °C.

Table 2. Selected bond lengths (Å) and angles (deg) for La_2CoMnO_6 and La_2NiMnO_6 at ambient temperature.

		La_2CoMnO_6	
TM	TM–O (Å)	No of bonds	O–TM–O (deg)
Co	2.071(4)	2	180.0
Co	2.014(5)	2	
Co	2.032(7)	2	
Mn	1.884(5)	2	180.0
Mn	1.934(4)	4	
		La_2NiMnO_6	
Ni	2.011(5)	2	179.97
Ni	1.976(6)	2	
Ni	2.016(9)	2	
Mn	1.88(5)	2	179.98
Mn	1.983(6)	2	
Mn	1.908(4)	2	

respectively. The unit cell parameters, atomic positions, thermal parameters and structure refinement details are given in table 3. Selected interatomic distances and angles are given in table 4. As in the low-temperature phases, charge ordering was confirmed to be present.

When heated to 25 °C below the transition temperature observed in the DSC, La_2NiMnO_6 was found to be present as a monoclinic, monophasic material. In contrast, the diffraction pattern of La_2CoMnO_6 was far more complex showing the simultaneous presence of both the low-temperature monoclinic and high-temperature rhombohedral phases. These differences

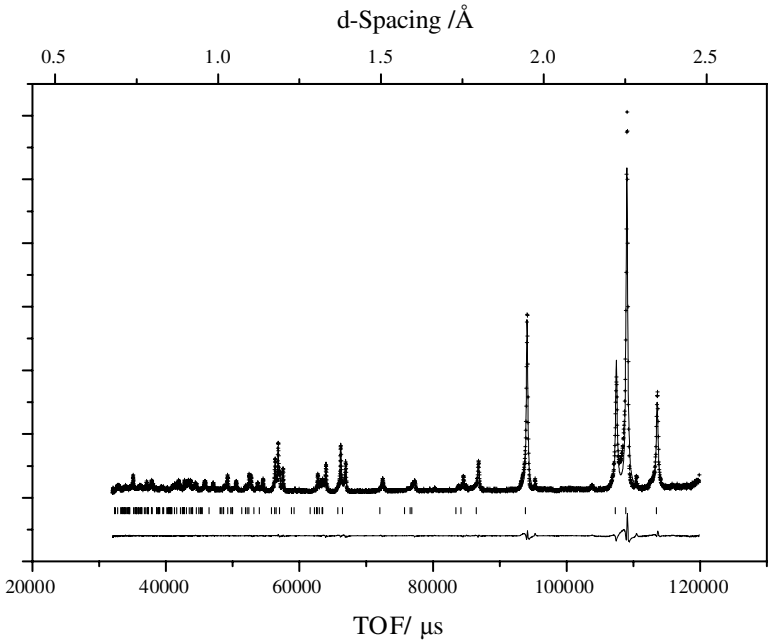

Figure 3. The neutron observed (+) and calculated (——) profile and difference profiles (bottom trace) for La_2CoMnO_6 at 375 °C.

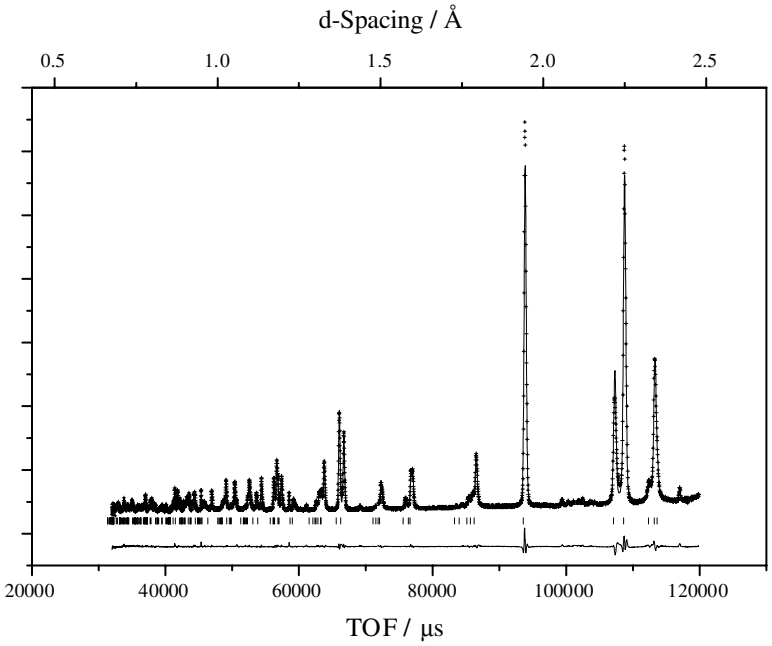

Figure 4. The neutron observed (+) and calculated (——) profile and difference profiles (bottom trace) for La_2NiMnO_6 at 400 °C.

may be related to the extended tail on the low-temperature side of the DSC peak in La_2CoMnO_6. Due to constraints on the neutron diffraction time available, we were unable to collect data of sufficient quality to allow Rietveld analysis of these materials.

Table 3. Results of Rietveld Refinement of neutron diffraction data for La_2NiMnO_6 and La_2CoMnO_6 at 350 and 400 °C respectively.

Parameter	La_2NiMnO_6	La_2CoMnO_6
Space group	$R\bar{3}$	$R\bar{3}$
a (Å)	5.474 56(16)	5.487 977(16)
b (Å)	5.474 56(16)	5.487 977(16)
c (Å)	5.474 56(16)	5.487 977(16)
α (deg)	60.6712(8)	60.7239(9)
β (deg)	60.6712(8)	60.7239(9)
γ (deg)	60.6712(8)	60.7239(9)
La x	0.249 64(21)	0.250 19(4)
y	0.249 64(21)	0.250 19(4)
z	0.249 64(21)	0.250 19(4)
U_{iso} (Å^2)	0.011 98(10)	0.011 55(8)
Co/Ni x	0	0
y	0	0
z	0	0
U_{iso} (Å^2)	0.018 59(6)	0.016 26(5)
Mn x	0.5	0.5
y	0.5	0.5
z	0.5	0.5
U_{iso} (Å^2)	0.018 59(12)	0.016 26(5)
O x	0.797 82(4)	0.800 11(8)
y	0.691 73(5)	0.687 28(8)
z	0.251 16(6)	0.256 40(12)
U_{iso} (Å^2)	0.020 25(8)	0.020 77(11)
Ni/Co:Mn ordering (%)	85	80
R_p (%)	4.92	10.78
wR_p (%)	6.28	12.1
χ^2	17.31	10.03

Table 4. Selected bond lengths (Å) and angles (deg) for La_2CoMnO_6 and La_2NiMnO_6 at 350 and 400 °C respectively.

La_2CoMnO_6			
TM	TM–O (Å)	No of bonds	O–TM–O (deg)
Co	2.024(5)	6	180
Mn	1.927(9)	6	180
La_2NiMnO_6			
Ni	2.0074(4)	6	180
Mn	1.928(6)	6	180

4. Discussion

Rietveld analysis of both La_2CoMnO_6 and La_2NiMnO_6 at ambient temperature indicated that the two TMs have a distinct preference (85%) for either the 2b (Mn) or 2c (Co/Ni) sites. Irrespective of the starting ratios used for the mixing of these sites, the refinement always converged to the same value. The observed site preference indicates that Mn–O–Co or Mn–O–Ni linkages predominate throughout the samples, giving to our knowledge the first direct proof of cation ordering in these materials. Further evidence for cation ordering is seen by

comparing the calculated M–O distances for each site (tables 2 and 4) which show significant differences, whereas if the TM ions were randomly distributed across these sites, an equal and averaged distance of about 1.95 Å for the M–O octahedra would be expected [24]. The observed TM–O distances are also very close to those obtained from EXAFS experiments [1, 2]. Close inspection of the high-temperature data (table 3) shows that in the rhombohedral symmetry the Co/Ni and Mn TMs show a site preference for the 1a and 1b sites respectively. The M site preference was maintained despite the first-order phase transition and the structural rearrangement necessary during the transformation from monoclinic to rhombohedral phase.

The degree of distortion around the MnO_6 octahedra in La_2NiMnO_6 is interesting. A large difference in the Mn–O bond lengths is observed between the long apical (1.983 Å) and basal bonds (1.903 and 1.88 Å) in the same octahedra. A similar degree of distortion been reported previously for $LaMnO_3$ [20], which is proposed to be due to a Jahn–Teller distortion. For $LaMnO_3$, the reported Mn–O distances are 1.918, 2.145 and 1.973 Å which are very similar to those observed in La_2NiMnO_6. The Jahn–Teller distortion occurs due to removal of the orbital degeneracy of a Mn^{3+} ion with an electronic configuration $t_g^3\, e_g^1$. The observed distortions in the Mn–O octahedra are consistent with the manganese ions being present in La_2NiMnO_6 as Mn^{3+} Jahn–Teller distorted. Thus, in order to maintain a neutral charge, the nickel ion must also be in the +3 formal oxidation-state. No such octahedral distortion was observed for the Mn–O octahedra in La_2CoMnO_6 and furthermore the average Mn–O bond distance is significantly shorter (1.89 Å), suggesting that manganese is in the +4 formal oxidation state. To maintain charge neutrality we would therefore expect Co to be in the +2 oxidation state, which can be inferred from the average Co–O bond distance (1.99 Å). The assignments of the oxidation states can also be confirmed from comparison of the L-edge x-ray absorption near edge structure (XANES) positions of these materials with standards of known oxidation state [25].

Even for the high-temperature phases after the transformation to rhombohedral symmetry, the cation ordering is maintained as shown by the site preference and the TM–O distances. However, there appears to be a loss of the Jahn–Teller distortion in the MnO_6 octahedra in La_2NiMnO_6. However, it is not possible to quantify this due to the larger isotropic displacement parameters for these high-temperature phases.

The transition from monoclinic to rhombohedral symmetry is a first-order phase transition. However, it has a diffuse nature in the case of La_2CoMnO_6. Both the monoclinic and rhombohedral phases coexist over a wide temperature range as observed in the ferroelectric $BaTiO_3$ [11] which has been reported to be a result of the particle size distribution [26]. Similar effects have been observed in PLZT (Pb, La)(Zr, Ti)O_3 over a temperature range where the cubic phase and tetragonal phase coexist [27]. Such diffuse phase transitions are usually observed in materials with mixed cation occupation as observed in this system. Indeed, we have also observed the coexistence of the two phases until about 100 °C below the transition temperature upon cooling. Interestingly, the work of Goodenough *et al* [8] reported this anomaly at room temperature; however, this may be due to quenching of this material from high temperature. We note that there is also a slightly high χ^2 value which may also be due to some unindexed peaks due to a small secondary phase or peak broadening a result of particle size or stress strain broadening.

5. Conclusions

Using TOF neutron diffraction we have shown, for the first time to our knowledge, that cation ordering exists in La_2NiMnO_6 and La_2CoMnO_6. The results of the Rietveld analyses have also enabled us to determine the oxidation states of the TM ions and show the degree of distortion within the octahedra (indicating the presence of Jahn–Teller distortion of the Mn^{3+} ion in

La_2NiMnO_6). We have also for the first time observed a temperature-driven first-order phase transition in these types of material.

Acknowledgments

CLB wishes to thank DERA for the studentship which funded this work. The authors also wish to thank EPSRC and CCLRC for providing access to the large-scale facility through the direct access route. The authors also wish to thank Professor C R A Catlow, Professor G D Price, Dr I G Wood, Dr G Sankar and Dr R Mortimer for their supervision and help in this project. Marrianne Odhlya (ULIRS) is also acknowledged for help in obtaining the DSC measurements.

References

[1] Bull C L 2001 *PhD Thesis* University of London
[2] Bull C L, Mortimer R, Sankar G, Gleeson D, Catlow C R A, Wood I and Price G D 2001 *Synth. Met.* **121** 1467
[3] Rajeev K, Vasanthacharaya N, Raychaudhuri A, Ganguly P and Rao C N R 1988 *Physica* C **153** 1331
[4] Du S, Wang J, Zheng H and Ma F 1993 *React. Kinet. Catal. Lett.* **51** 415
[5] Ganguly P, Vasanthacharaya N, Rao C N R and Edwards P 1984 *J. Solid State Chem.* **54** 400
[6] Narasinman V, Keer H and Chakrabarty D 1985 *Phys. Status Solidi* a **89** 65
[7] Wu Y, Yu Z and Liu S 1994 *J. Solid State Chem.* **112** 157
[8] Goodenough J B, Wold A, Arnold R J and Menyuk N 1961 *Phys. Rev.* **124** 373
[9] Rao C N R, Arulraig A, Cheetham A K and Naveau B 2000 *J. Phys.: Condens. Matter* **12** B83
[10] Asai K, Fujiyoshi K, Nishimori N, Satoh Y, Kobayashi Y and Mizoguchi M 1998 *J. Phys. Soc. Japan* **67** 4218
[11] Westphal V, Heem W and Glincluck M 1992 *Phys. Rev. Lett.* **68** 847
[12] Sears V K 1992 *Neutron News* **3** 29
[13] Asai K, Sekizawa H and Iida S 1979 *J. Phys. Soc. Japan* **47** 4
[14] Troyanchuk I, Samsoneuko N, Kasper N, Szymczah H and Nabialeh A 1997 *J. Phys.: Condens. Matter* **9** 287
[15] Wold A, Arnold R J and Goodenough J B 1958 *J. Appl. Phys.* **29** 387
[16] Mortimer R, Powell J and Vasanthacharaya N 1997 *J. Phys.: Condens. Matter* **9** 11209
[17] Larson A G and von Dreele R 1987 *GSAS Manual, Los Alamos Report No* LA-UR-86-748
[18] Werner P E, Eriksson L and Westdahl M 1985 *J. Appl. Crystallogr.* **18** 367
[19] LeBail A, Duroy H and Fourquet J L 1988 *Mater. Res. Bull.* **23** 447
[20] Garcia Munoz J, Suaaidi M, Foutcuberta J and Rodriguez Carvajal J 1997 *Phys. Rev.* B **55** 34
[21] David W I F and von Dreele R, unpublished results
[22] Ikeda S and Carpenter J M 1985 *Nucl. Instrum. Methods* A **239** 536
[23] Woodward P 1997 *Acta Crystallogr.* B **53** 32
[24] Shannon R D 1976 *Acta Crystallogr.* A **32** 751
[25] Bull C L, Mortimer R, Sankar G, Gleeson D, Catlow C R A and Price G D 2003 in preparation
[26] Park Y, Lee W and Kim H 1997 *J. Phys.: Condens. Matter* **9** 9445
[27] Strenger C and Burrgraef A 1980 *J. Phys. Chem. Solids* **41** 17